Transition-State Characterization of the Ammonia Ionization Process in Aqueous Solution via the Free-Energy Gradient Method

Masataka Nagaoka,* Yukihiko Nagae, Yoshiyuki Koyano, and Yuki Oishi

Graduate School of Information Science, Nagoya University, Furo-cho, Chikusa-ku, Nagoya 464-8601, Japan

Received: October 25, 2005; In Final Form: February 8, 2006

For the ionization process of ammonia in aqueous solution, the transition-state (TS) structure was fully optimized for the first time on the free-energy surface (FES) by applying the free-energy gradient (FEG) method combined with a hybrid quantum mechanical and molecular mechanical molecular dynamics (QM/MM-MD) method. In aqueous solution, the ionization process was found to proceed by way of a clear TS (R(N1−H5) = 1.512 Å), which does not exist in the gas phase. The free-energy (FE) of activation for ionization obtained was 14.7 kcal/mol, within the classical approximation, via the QM/MM-MD FEG method, and is found to be in good agreement with 9.57 kcal/mol estimated from the TS theory using the experimental value of the rate constant. Apart from the dynamic correction, it is indicated that the theoretical value would be improved to be 10.28 kcal/mol if the electronic-state calculation could be executed at the B3LYP/6-31G(d) level of theory.

1. Introduction

In a lot of chemical, biological, and environmental phenomena there is no room for doubt about such a fact that the chemical reaction dynamics *in solution* plays a very important role, where the microscopic solvation structures of solute molecules offer essential and inevitable information. Development of theoretical methods to know stable or transition states *in solution* is, therefore, a crucial issue for deeply understanding these phenomena.[1−15] However, by the necessity of taking a large number of solvent molecules into consideration, there are several theoretical restrictions to study even equilibrium thermodynamic characteristics of chemical reactions *in solution*.

Until now, a number of theoretical methods have been applied to solution chemistry.[1−15] Among them, on the basis of the recent theoretical advancement,[1−20] the free-energy gradient (FEG) method was invented and has been developed[9−15] with applications to identify not only stable states (SS) of molecular structures[12,14] but also their transition states (TS) *in solution*,[13] where *full structural optimizations* were executed with respect to all of the degrees of freedom of a solute molecule, for example, SS of a glycine and its TS of ionization,[10−12] TS in a Menshutkin reaction[13] and SS of an ammonia−water ($H_3N\cdots H_2O$) molecule pair in aqueous solution.[14,15] Being analogous to the energy gradient method on the Born−Oppenheimer potential energy surface (BO-PES) in molecular orbital (MO) theory, the FEG method utilizes the force on the free-energy surface (FES).[9] In fact, one can calculate the force on FES by the time-average of the sum of forces acting instantaneously on each constituent atom of a solute molecule with respect to all of the solvent molecules. As a matter of fact, if one noticed that these forces are necessarily calculated at each time-step increment in the MD simulation, he/she could find no other useful way more plausible than utilizing them.

It is worth mentioning that Aguilar et al. have been recently applying the FEG method successfully to optimize molecular geometries in solution in combination with their developed mean field approximation, that is, the average solvent electrostatic potential (ASEP).[21,22] It has such a merit that "ab initio" electronic state calculation could be utilized for reactant molecules because the FE derivatives can be evaluated simply by using ASEP for the purpose of accomplishing the computational efficiency. In general, the FEG method with the ASEP/MD method should be applied successfully to such solution systems where the instantaneous solvent polarization might not influence seriously on chemical reactions.

In this article, we take the ammonia ionization process in aqueous solution as an application example to execute the *full-atomic* TS optimization within the framework of the FEG method.[14] The model charge separation reaction, that is, $H_3N-HOH \rightarrow H_3N-H^+ + O^-H$, is really the "first" example of the FEG method that does not have a "TS" by itself, just leading to the unstable products, but does clearly in solution. Ammonia was chosen because, among a lot of small molecules, it is a fundamental molecule and has such interesting characteristics that the gas species shows extremely high solubility into water, that is, 612.7 NH_3(g)mL/H_2O(l)mL[23] and forms the surface-bound state on the ice surface.[24−26] It is, therefore, important to know the hydrated structure and the ionization process of ammonia in water because it also leads directly to understanding the solution structure of ammonia aqueous solution in its dense state. In the present study, taking into consideration the previous study of ammonia−water clusters[27−30] and thermodynamic experiments,[30−33] the TS structure for the ionization process of an ammonia molecule in aqueous solution is studied theoretically and presented, for the "first" time, as a concrete structural form of $H_3N\cdots H_2O$ molecule pair in use of the FEG method combined with a hybrid quantum mechanical and molecular mechanical molecular dynamics (QM/MM-MD) method. In addition, the characteristic difference between the present method and the COSMO one is comparatively discussed, showing how the microscopic contributions of both internal

* Corresponding author. E-mail: mnagaoka@is.nagoya-u.ac.jp. URL: http://frontier.ncube.human.nagoya-u.ac.jp/. Tel & Fax: +81-52-789-5623.

10.1021/jp056115c CCC: $33.50
Published on Web 03/15/2006

energy and entropy to free energy play their own roles in solution chemical reaction, especially in the ammonia ionization reaction.

This article is organized as follows: First, in the following section, theory and computational methods are explained: (i) QM/MM method, (ii) FEG method and (iii) computational detail. In the third section, we will provide a number of results and discussion with respect to (i) structure optimization of TS on FES and (ii) FE of ionization. Finally, in the last section, concluding remarks are provided.

2. Theory and Computational Methods

2.1. QM/MM Method. The QM/MM method is adopted to describe the ammonia ionization process in aqueous solution for the purpose of including explicitly the influence of solvent water microscopic structure into the solute $H_3N\cdots H_2O$ pair electronic state.[17−20,34] Then, the effective Hamiltonian consists of the quantum mechanical (QM) term $\hat{H}_{QM}$, the interaction term $\hat{H}_{QM/MM}$ between the QM and the molecular mechanical (MM) system, and the pure MM term $\hat{H}_{MM}$

$$\hat{H} = \hat{H}_{QM} + \hat{H}_{QM/MM} + \hat{H}_{MM} \tag{2.1}$$

In this article, $\hat{H}_{QM/MM}$ describes the solute−solvent QM/MM interaction, which is defined as a sum of (i) electrostatic and (ii) *non*electrostatic (van der Waals) contributions

$$\hat{H}_{QM/MM} = \hat{H}^{elec}_{QM/MM} + \hat{H}^{vdW}_{QM/MM} \tag{2.2}$$

where

$$\hat{H}^{elec}_{QM/MM} = \sum_M q_M V_{QM}(\mathbf{R}_M) \tag{2.3}$$

with

$$V_{QM}(\mathbf{R}_M) = -\sum_i \frac{1}{r_{iM}} + \sum_A \frac{Z_A}{R_{AM}} \tag{2.4}$$

and

$$\hat{H}^{vdW}_{QM/MM} = \sum_A \sum_M \left(\frac{A_{AM}}{R^{12}_{AM}} - \frac{B_{AM}}{R^{6}_{AM}} \right) \tag{2.5}$$

In these expressions, q_M is the atomic point charge on the Mth MM atom located at $\mathbf{R}_M$ in solvent water molecules, r_{iM} is the distance between the ith QM electron and the Mth MM atom, Z_A is the core charge of the Ath QM atom in the $H_3N\cdots H_2O$ pair, R_{AM} is the distance between the Ath QM atom and the Mth MM one, and A_{AM} and B_{AM} are a couple of Lennard-Jones parameters for the Ath QM atom interacting with the Mth MM atom. The total system potential energy V is, thus, expressed as follows

$$V = \langle \Psi | \hat{H}_{QM} + H_{QM/MM} | \Psi \rangle + V_{MM} \tag{2.6}$$

$$= V_S + \langle \Psi | \hat{H}_{QM/MM} | \Psi \rangle + V_{MM} \tag{2.7}$$

$$= V_{SB} + V_{MM} \tag{2.8}$$

where $|\Psi\rangle$ denotes an instantaneous SCF wave function of electrons at an $H_3N\cdots H_2O$ structure $\mathbf{q}^s$ in solution

$$[\hat{H}_{QM}(\mathbf{q}^S) + \hat{H}_{QM/MM}(\mathbf{q}^S;\mathbf{q}^B)]|\Psi\rangle = V_{SB}|\Psi\rangle \tag{2.9}$$

where $\mathbf{q}^B$ denotes an instantaneous configuration of solvent molecules as a whole, and V_{SB} is the instantaneous eigenvalue and is equal to the sum of solute potential energy, V_S, and solute−solvent interaction energy at $\mathbf{q}^s$.

For comparison, the conductor-like screening model (COSMO) method[35] is also used, where the water solvent is treated as a continuum material with a characteristic dielectric constant ϵ (78.4 for water), and the introduction of a solute molecule-shaped cavity of the solvent leads to a quite quantitative description of the solvation phenomenon.

2.2. Free-Energy Gradient Method. The FE difference ΔA_i is expressed, by the free-energy perturbation (FEP) theory,[36,37] as follows

$$\Delta A_i = A_{i+1} - A_i = -k_B T \ln\langle \exp[-\beta\{V_{SB}(\mathbf{q}^s_{i+1}) - V_{SB}(\mathbf{q}^s_i)\}]\rangle_i \tag{2.10}$$

where, $\mathbf{q}^s_i$ is the ith solute structure, that is, a structure of $H_3N\cdots H_2O$ 1:1 pair, and $\mathbf{q}^s_{i+1}$ is the i + first structure that is accessible perturbatively from $\mathbf{q}^s_i$. The brackets $\langle\cdots\rangle_i$ in eq 2.10 denote the equilibrium ensemble average

$$\langle\cdots\rangle_i = \frac{\int d\mathbf{q}^B(\cdots)\exp(-\beta V(\mathbf{q}^S_i))}{\int d\mathbf{q}^B \exp(-\beta V(\mathbf{q}^S_i))} \tag{2.11}$$

where V is the whole system potential energy (eq 2.6). The subscript i in the average $\langle\cdots\rangle_i$ in eq 2.10 means that it has taken over the sampling at $\mathbf{q}^s_i$.

In MD simulation, the forces acting on all of the atoms in a solute molecule by all of the solvent molecules are calculated every time step of numerical integration. In particular, in equilibrium MD simulation, by time-averaging instantaneous forces against a constrained structural solute molecule by all of the solvent molecules, the force on FES, $\mathbf{F}^{FE}(\mathbf{q}^S_i)$, that is, a minus of FEG, is obtained as a function of $\mathbf{q}^S_i$,[9]

$$\mathbf{F}^{FE}(\mathbf{q}^S_i) = -\frac{\partial A(\mathbf{q}^S_i)}{\partial \mathbf{q}^s} = -\left\langle \frac{\partial V_{SB}(\mathbf{q}^S_i)}{\partial \mathbf{q}^s} \right\rangle \tag{2.12}$$

where $A(\mathbf{q}^S_i)$ is the Helmholtz free-energy function under the thermodynamic condition (N, V, T) and the brackets $\langle\cdots\rangle$ in eq 2.12 denote the time average, under the equilibrium condition, that is equal to the equilibrium ensemble average (eq 2.11) under the condition that the $H_3N\cdots H_2O$ pair structure is fixed to be $\mathbf{q}^S_i$.

In use of $\mathbf{F}^{FE}(\mathbf{q}^s)$, we adopt here the Euler method for geometry optimization[38,39] and the TS structure of $H_3N\cdots H_2O$ in aqueous solution is optimized with respect to all coordinates after the optimization for the reaction coordinate R(N−H) in the linear N···H−O hydrogen bond. The Euler method is the simplest steepest descent method where only the gradient is used to determine the displacement vector $\Delta\mathbf{q}^s_i$.[38] Currently, taking into consideration the fact that the short-time solution of Newtonian equation of motion is obtained

$$\mathbf{q}^S(t+\Delta t) = \mathbf{q}^S(t) + \frac{d\mathbf{q}^S(t)}{dt}\Delta t + \frac{1}{2}\mathbf{M}^{-1}\cdot\mathbf{F}(t)(\Delta t)^2 \tag{2.13}$$

a simple definition of displacement vector

$$\Delta\mathbf{q}^s_i \equiv c_i \mathbf{M}^{-1}\cdot\mathbf{F}^{FE}_i \tag{2.14}$$

is taken by multiplying

$$\mathbf{F}_i^{\mathrm{FE}} \equiv \mathbf{F}^{\mathrm{FE}}(\mathbf{q}_i^{\mathrm{s}}) = -\left\langle \frac{\partial V_{\mathrm{SB}}(\mathbf{q}^{\mathrm{s}})}{\partial \mathbf{q}^{\mathrm{s}}} \right\rangle_i \tag{2.15}$$

by an adaptive constant c_i of dimension T^2 and the inverse of the constant mass matrix

$$\mathbf{M} = \begin{pmatrix} m_1 & & & & & & \mathbf{0} \\ & m_1 & & & & & \\ & & m_1 & & & & \\ & & & \ddots & & & \\ & & & & m_7 & & \\ & & & & & m_7 & \\ \mathbf{0} & & & & & & m_7 \end{pmatrix} \tag{2.16}$$

In eq 2.14, because the matrix $\mathbf{M}$ is constant, only c_i is optimized to minimize $A(\mathbf{q}_i^{\mathrm{S}} + c_i \mathbf{M}^{-1}\cdot\mathbf{F}_i^{\mathrm{FE}})$ by a sequence of one-dimensional searches.

Thus, the procedure in the FEG method is executed as follows:

(P1) Start with the geometry $\mathbf{q}_k^{\mathrm{s}}$, $k = 0$.

(P2) Find the stationary point using the force on the FES $\mathbf{F}_k^{\mathrm{FE}}$, and determine the adaptive displacement vector

$$\Delta\mathbf{q}_k^{\mathrm{s}} = c_k \mathbf{M}^{-1}\cdot\mathbf{F}_k^{\mathrm{FE}} \tag{2.17}$$

searching the optimum c_k.

(P3) For $\mathbf{q}_k^{\mathrm{s}}$, calculate the FE change ΔA_k by eq 2.10 in the FEP theory.

If the force $\mathbf{F}_k^{\mathrm{FE}}$ is small enough within the tolerance of convergence and/or the predicted change in the geometry $\Delta\mathbf{q}_k^{\mathrm{s}}$ is small enough to be satisfied with the condition

$$\left\langle \frac{\partial V_{\mathrm{SB}}(\mathbf{q}^{\mathrm{s}})}{\partial \mathbf{q}^{\mathrm{s}}} \right\rangle_k \approx 0; \quad \text{zero-gradient condition} \tag{2.18}$$

then stop.

(P4) Set $\mathbf{q}_{k+1}^{\mathrm{s}} = \mathbf{q}_k^{\mathrm{s}} + \Delta\mathbf{q}_k^{\mathrm{s}}$, $k = k + 1$ and return to step P2. Using the FE change ΔA_k thus determined at each step, the FE difference between the reactant state and TS, $\Delta A^{\ddagger}$, can be obtained by

$$\Delta A^{\ddagger} = \sum_{k=0}^{N} \Delta A_k \tag{2.19}$$

where $k = 0$ and N designate the reactant and TS state, respectively. In this study, a number of successive states are parametrized by the distance R(N−H) between the nitrogen atom of ammonia molecule and the proton of a water molecule that is hydrogen-bonding to the nitrogen atom in the $H_3N\cdots H_2O$ molecule pair. Hereafter, the present path-following procedure with an adaptive constant c_i is called the *adaptive steepest-descent-path scheme*.[14]

It is worth mentioning that at an optimized structure, in addition to the zero-gradient condition eq 2.18, the following *force-balance condition* must be fulfilled:[14]

$$\left\langle \frac{\partial V_{\mathrm{S}}(\mathbf{q}^{\mathrm{S}})}{\partial \mathbf{q}^{\mathrm{S}}} \right\rangle = \left\langle \frac{\partial \langle\Psi|\hat{H}_{\mathrm{QM}}|\Psi\rangle}{\partial \mathbf{q}^{\mathrm{S}}} \right\rangle = -\left\langle \frac{\partial \langle\Psi|\hat{H}_{\mathrm{QM/MM}}|\Psi\rangle}{\partial \mathbf{q}^{\mathrm{S}}} \right\rangle \tag{2.20}$$

because the free-energetical optimization is accomplished in compensation for the balance between the solute potential energy gradient and the forces acting on each solute atom due to solvation. Precisely in Figure 1, this is a force balance between the restoring force on nuclei, which is to return back to the charge distribution of the bare solute molecule, that is, $+\mathbf{f}$, and the force executed by solvent toward the charge distribution, that is, $-\mathbf{f}$. Even if the geometrical change might be small in solution, the mechanism that maintains it microscopically could be fully different.

2.3. Computational Details. For the whole system including a QM system that contains a couple of reactant molecules, that is, an ammonia and a water molecule, and 241 MM water molecules, MD calculations were carried out in a cubic simulation box ($19.34 \times 19.34 \times 19.34$ Å^3) under the periodic boundary condition in use of ROAR 2.0 program[40,41] modified partly for the present purpose. The velocity-Verlet algorithm was used with the RATTLE scheme for the geometry constraint of the $NH_3\cdots H_2O$ pair,[42,43] and the simultaneous equations of motion were solved numerically with a time step 0.1 fs and the nonbonded cutoff distance 9.0 Å. After 5000-step simulation for equilibration, a sampling run was executed for 30 000 steps ($= 3 \times 10^4$ configurations) and was used to calculate physical quantities by averaging over this equilibrium sampling. The temperature was kept at 300 K with the Nosé−Hoover chain algorithm,[44] and the system was maintained to be a canonical (NVT) ensemble. As a result, the mass density in the box was prepared to be 1.0001 g/cm^3.

For the $H_3N\cdots H_2O$ molecule pair (the QM portion), $\hat{H}_{\mathrm{QM}}$ was treated at the PM3 level of theory[45−47] for describing the ionization reaction to give $NH_4^+\cdots OH^-$, while solvent water molecules (the MM portion) were described by the TIP3P rigid water model.[48] For the Lennard-Jones-type interaction between QM and MM atoms, we have used those parameters developed by Ruiz-López's group especially for a couple of QM ammonia and TIP3P water molecules and a couple of QM and TIP3P water molecules,[34,49] where the structural and energetic properties of the QM/MM interaction were adjusted to reproduce the reference values computed at the level of the B3LYP density functional method[50] with the 6-31G(d) basis, which gives a reliable description of electrostatic properties[51] and of structural and energetic features of hydrogen-bonded complexes.[52] The interaction of the neutral pair $H_3N\cdots H_2O$ with the water solvent is well described by the TIP3P waters. However, its parametrization is also adequate enough for the description of interaction of water with the NH_4^+ and OH^- ions. This is because the TIP3P water has bare charge sites not only on the oxygen site (−0.834) but also on the hydrogen ones (+0.417) although the Lennard-Jones site is located only on the oxygen atom, and, further, because the NH_4^+ here is not isolated but with OH^- together that is behaving as a proton donor in the reaction.

The PM3 used currently was not reparametrized for the current application because in our preliminary investigation its native parametrization was considered reliable enough to describe proton transfer in the present ammonia/water system, reproducing reasonably the neutral $H_3N\cdots H_2O$ cluster structure, not obtained by AM1, and a similar potential curve for ionization that might be consistently higher than B3LYP/6-31G(d) by a few kcal/mol, though. In addition, for the present QM/MM parametrization, we followed ref 34 where they were calibrated to reproduce the level of theory of the B3LYP density functional

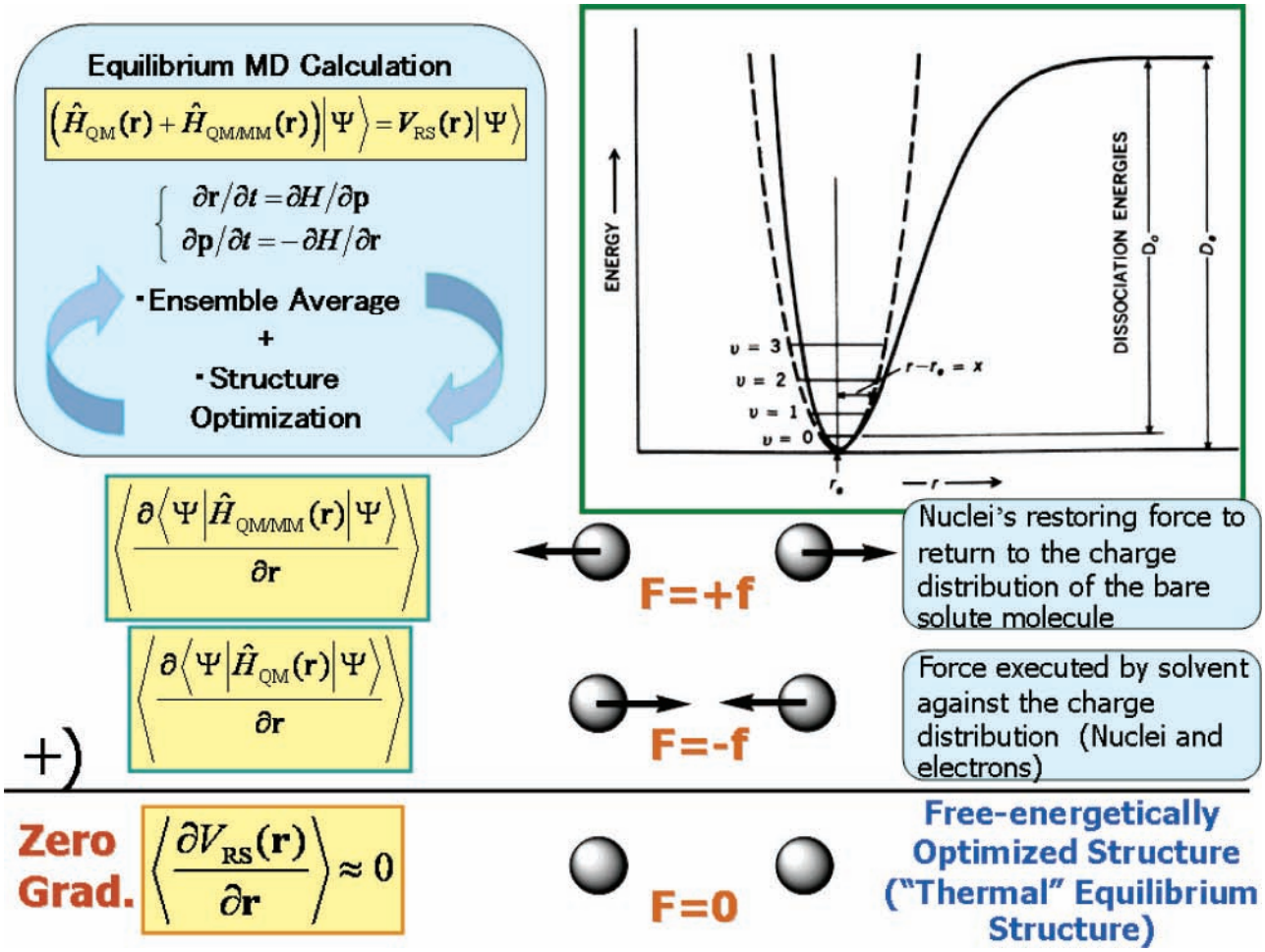

Figure 1. Schematic explanation of the force-balance condition: At the free-energetically optimized structure, the force-balance condition must be fulfilled in addition to the zero-gradient condition. This is a force balance between the restoring force on nuclei that is to return back to the charge distribution of the bare solute molecule, and the force executed by solvent toward the charge distribution.

method with the 6-31G(d) basis and were checked so that the profiles may exhibit the expected shapes for the Coulombic interaction energy. In fact, they roughly follow the shape of the reference B3LYP/TIP3P electrostatic energy profile, and there is general agreement between PM3/TIP3P and B3LYP/TIP3P profiles. This agreement was attained under such a policy originally set by Field et al. that the semiempirical parameters on QM atoms were left unchanged and only those on the MM sites were optimized.[19] So far, the suitability of semiempirical theory to treat QM/MM interactions has also been examined in numerous studies,[49,53,54] including recent development of modified PM3 methods with a parametrizable interaction function (PIM)[55a,c] for intermolecular interactions and with a method adapted for intermolecular studies (MAIS).[55b,c]

3. Results and Discussion

3.1. Transition-State Structure on the Free-Energy Surface. To obtain the optimized TS structure of $H_3N\cdots H_2O$ molecule pair in aqueous solution, we calculated the FE profile as a function of R(N1−H5) in the range from 1.812 Å to 1.392 Å by 0.03 Å decrement, optimizing all of the other structural parameters of the $H_3N\cdots H_2O$ molecule pair (Figure 2a). At each optimization step at a value of R(N1−H5), all of the relative atomic positions in the pair structure were updated along the direction of the average force vector $\mathbf{F}^{FE}(\mathbf{q}_i^s)$ by a displacement vector $\Delta\mathbf{q}_i^s$, which was chosen appropriately according to the *adaptive steepest-descent-path scheme*.[14] The resultant FE profile in aqueous solution is shown in the ● curve in Figure 2a. It should be noted that only one imaginary frequency was obtained at this structure by the *normal-mode analysis* on FES incorporated the effect from all of the ambient water molecules occurred by MD simulations. The average root-mean-square (RMS) force at the optimized TS geometry

$$\mathrm{rms}(\mathbf{F}_{TS}^{FE}(\mathbf{q}_{TS}^{S}))=\frac{1}{T}\int_0^T dt\sqrt{(\mathbf{F}_{TS}^{FE}(t))^2/3N_{atom}} \qquad (3.1)$$

was 0.0086 hartree/bohr, which is satisfactory in comparison with the value at the SS, that is, 0.0043 hartree/bohr,[14] and the previous values of SS for glycine zwitterion, that is, 0.0025 hartree/bohr,[12] and of TS for a Menshutkin reaction, that is, 0.0010 hartree/bohr,[13] in aqueous solution. Additionally in Figure 2a, also shown are the solute potential energy V_S changes in gas phase (○ (PM3) and □ (B3LYP/6-31G(d))) and that in aqueous solution by the COSMO method (▲).[35] All of the separate MO calculations were executed by GAUSSIAN03.[56] In eq 3.1, N_{atom} is the total number of atoms, that is, 7 for the present system, and the upper limit of time integral T is 3 ps (= 30 000 steps × 0.1 fs), that is, the time period for equilibrium MD simulation at a fixed structure of the $H_3N\cdots H_2O$ molecule pair.

The structure that corresponds to the maximum of the FE curve (A_{FEG}: ●) at R(N1−H5) = 1.512 Å in Figure 2a was taken to be the free-energetically optimized TS structure and is shown in Figure 3a together with the SS one (Figure 3b)

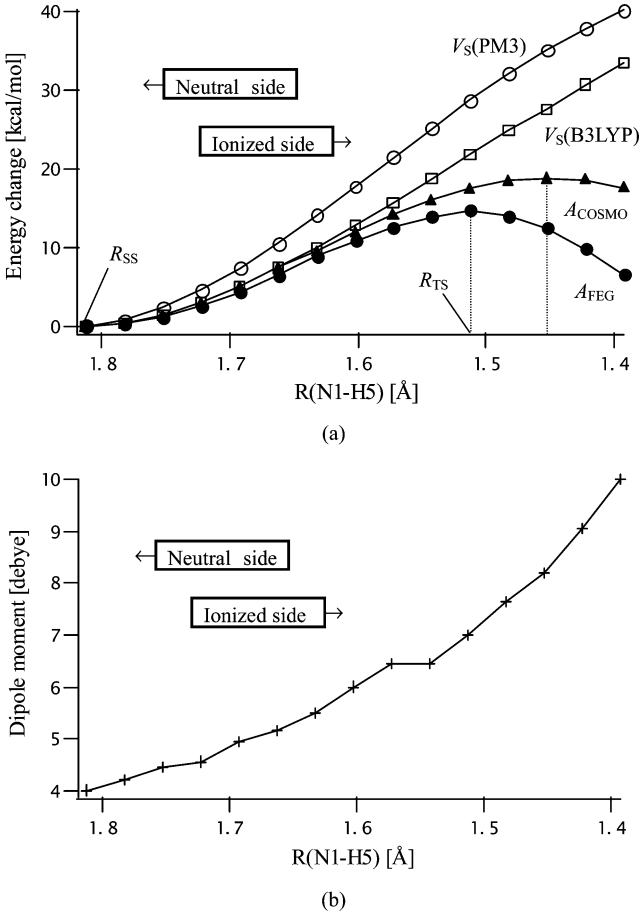

Figure 2. (a) Energy profiles in aqueous solution by the FEG method (A_{FEG}, closed circles: ●) and the COSMO method (A_{COSMO}, closed triangles: ▲) and in the gas phase at the B3LYP/6-31G(d) (V_S(B3LYP), opened squares: □) and PM3 (V_S(PM3), opened circles: ○) level of theory along the reaction coordinate R(N1−H5) according to the FEG method. (b) Dipole moment change in aqueous solution along the reaction coordinate R(N1−H5) by the FEG method.

obtained in our previous work.[14] In addition, the structure by the COSMO method that corresponds to the maximum on the closed triangle curve (A_{COSMO}: ▲) at R(N1−H5) = 1.452 Å in Figure 2a is shown (Figure 3c). They all have the C_s symmetry. In the FES TS geometry (Figure 3a), it is obvious that the H5 atom is situated in the middle position between O6 and N1 for transformation from the polarized neutral state into an ionized one. In comparison to the SS structure (Figure 3b), the H5−O6−H7 angle, θ(H5−O6−H7), becomes slightly larger and R(O6−H7) becomes shorter in the TS structure (Figure 3a) because of the transformation of the H_2O molecule to OH^- and H^+ ions. Alternatively, in comparison to R(N1−O6) = 2.792 Å at the TS structure by the COSMO method (Figure 3c), it is found that R(N1−O6) becomes longer at the structure by the FEG method (Figure 3a), that is, 2.820 Å.

The dipole moment change of the $H_3N\cdots H_2O$ 1:1 pair in aqueous solution was calculated along the reaction coordinate R(N1−H5) by the FEG method (Figure 2b). It is recognized that as R(N1−H5) becomes shorter the dipole moment becomes larger according to the ionization progress. From Figure 2a and b, it is shown clearly that the H_3N-H_2O pair in aqueous solution is free-energetically stabilized by ambient water molecules, although the pair's polarization makes the bare potential energy increase. However, at those two structures that correspond to two maxima of the energy curves ● and ▲ in Figure 2a, that is, R(N1−H5) = 1.512 Å in the FEG method and 1.452 Å in the

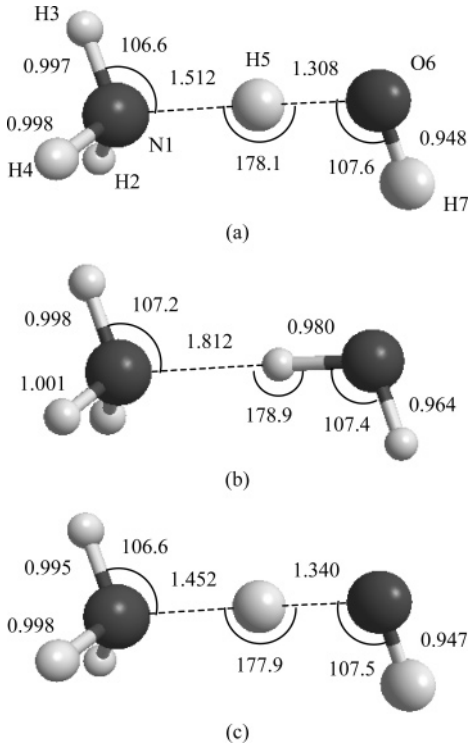

Figure 3. Optimized geometries of the $HN_3\cdots H_2O$ molecule pair in aqueous solution at (a) the transition state and (b) the stable state by the FEG method, and (c) that corresponding to the maximum of the energy curve in aqueous solution by the COSMO method in Figure 1a. Bond lengths are in Angstroms and bond angles are in degrees.

COSMO one, it was found that the dipole moment of the latter method, that is, 8.218 D, is larger than that of the former method, that is, 7.032 D (Table 1). Such a large difference in dipole moments is connected closely to the difference of stabilization estimate between the FEG and COSMO methods.

3.2. Radial Distribution Functions and the Solvation Structures. In Figure 4a−c, shown are the radial distribution functions (RDFs) $g(R)$s with respect to the N1−OW, H5−OW, and O6−OW distances at SS (R(N1−H5) = 1.812 Å) and TS (R(N1−H5) = 1.512 Å), respectively, where OW is the abbreviation of the oxygen atoms of solvent water molecules. Potentials of mean force (PMFs) $w(R)$s, that is, $w(R) = -k_BT$ ln $g(R)$, are also drawn in the unit of k_BT (T = 300 K). It was obvious that the sharper enhancement and the shorter-side shifting of both peaks with respect to the N1−OW (Figure 4a) and the O6−OW (Figure 4c) distances at TS are a direct evidence of the stronger solvation brought about by the larger absolute values of gross atomic charges of NH_3 and $O^{\delta-}$ H at TS, that is, +0.152 and −0.381 (cf. +0.037 and −0.262 at SS) (Table 1). However, one can notice in Figure 4b that the first peak of RDF at TS shifts a little to the longer side with respect to the H5−OW distance and becomes rather broader than that at SS. This is understandable because the atomic charge of the transferring proton H5 stays almost unchanged, that is, +0.228 at TS and +0.226 at SS (Table 1).

3.3. "Free Energy" Evaluation − COSMO versus FEG. It is the TS structural difference that makes the dipole moment in the COSMO method larger than that in the FEG method. The "free energy" calculation is achieved, in the COSMO method, only on the basis of "enthalpy", thus leading to the following expression of "free energy" of activation

$$\Delta A^{\ddagger}_{COSMO} = A_{COSMO}(R_{TS}) - A_{COSMO}(R_{SS}) \qquad (3.2)$$

TABLE 1: Atomic Charges and Dipole Moments of the Bare NH_3-H_2O Molecule Pair at SS and TS Structure in Aqueous Solution

	SS (R(N1−H5) = 1.812 Å)		TS (R(N1−H5) = 1.512 Å)		
	PM3	B3LYP/6-31G(d)	PM3	B3LYP/6-31G(d)	MP2/6-31G(d)
N1	−0.066	−0.907	0.063	−0.908	−1.054
H2	0.032	0.317	0.028	0.345	0.384
H3	0.033	0.318	0.033	0.351	0.389
H4	0.038	0.324	0.028	0.346	0.384
H5	0.226	0.432	0.228	0.389	0.489
O6	−0.436	−0.845	−0.550	−0.866	−0.980
H7	0.174	0.361	0.169	0.343	0.387
μ^a	3.485	4.178	5.027	5.834	6.082
	FEG(PM3) 4.004[b]	COSMO(PM3) 4.109[b]	FEG(PM3) 7.032[c]	COSMO(PM3) (R(N1−H5) = 1.452 Å) 8.212[c]	

[a] Expressed in Debye. [b] Reference 14. [c] Dipole moments are also shown for the FEG and COSMO methods with the PM3 level of theory.

$$\cong \Delta H^{\ddagger}_{\mathrm{COSMO}} \tag{3.3}$$

$$= H_{\epsilon}(R_{\mathrm{TS}}) - H_{\epsilon}(R_{\mathrm{SS}}) = \Delta H^{\ddagger}_{\epsilon} \tag{3.4}$$

where $\Delta H^{\ddagger}_{\mathrm{COSMO}}$ is the COSMO energy of activation that is the difference between the heats of formation at R_{TS} and R_{SS}, $H_{\epsilon}(R_{\mathrm{TS}})$ and $H_{\epsilon}(R_{\mathrm{SS}})$, with the dielectric constant ϵ for water, that is, 78.4. This means that the larger dipole moment is simply advantageous in the enthalpic estimate of stabilization in the polar solvent not only for the SS structure but also for the TS one. Precisely, this tendency rises owing to the electronic polarization due to the solvent, namely, due to the "dielectric" hydration, despite the solute potential energy destabilization (Figure 2a and Table 1), which is consistent with the opinion about the induced dipole moment of water molecule in water.[57−59]

However, the stabilization in the FEG method is realized, in contrast, literally on the basis of FE, including legitimately the entropic contribution

$$\Delta A^{\ddagger}_{\mathrm{FEG}} = A_{\mathrm{FEG}}(R_{\mathrm{TS}}) - A_{\mathrm{FEG}}(R_{\mathrm{SS}}) \tag{3.5}$$

$$= \Delta U^{\ddagger}_{\mathrm{FEG}} - T\Delta S^{\ddagger}_{\mathrm{FEG}} \tag{3.6}$$

which counts in not only the dipole moment itself but also the relative orientation of ambient solvent molecules against the reactants, that is, the "microscopic" solvation internal energy (SIE) (NB, solvation enthalpy in the NPT ensemble) and the "microscopic" solvation entropy (SE),[12−15] in addition to their molecular structural changes themselves.

As a matter of fact, for such an ionization reaction of ammonia considered currently

$$H_3N\text{---}HOH \rightarrow H_3N\cdots H^{\delta+}\cdots O^{\delta-}H \rightarrow H_3N{-}H^{+} + O^{-}H \tag{3.7}$$

the entropy might increase or decrease as the reaction proceeds because the effect of unimolecularity lacking should compete with the charge separation increase that accompanies the microscopic structurization. The inner sharper first peaks in RDFs at TS (Figure 4a and c), as discussed in section 3.2, have shown that the whole solvated system at TS acquires a larger FE stabilization (as an amount of SIE) than that at SS, which might be estimated roughly from the differences between the first two minima in PMFs.[20b] In fact, this microscopic SIE stabilization should be the main portion of the FE stabilization. Thus, taking into account this microscopic SIE contribution, it can be assumed currently that

$$\Delta U^{\ddagger}_{\mathrm{FEG}} < \Delta H^{\ddagger}_{\epsilon} \tag{3.8}$$

because $\Delta H^{\ddagger}_{\epsilon}$ can include nothing but such a portion of SIE that can be treated insufficiently within the dielectric continuum model, whereas $\Delta U^{\ddagger}_{\mathrm{FEG}}$ can do additionally the microscopic SIE around individual reactant atoms, whose contribution should stabilize TS more in the present case.

However, with respect to the microscopic SE contribution, it can be expected that the entropy of activation, $\Delta S^{\ddagger}$, would become less than or, at most, almost equal to zero:

$$\Delta S^{\ddagger}_{\mathrm{FEG}} \leq 0 \tag{3.9}$$

because the partial entropy around N1 and O6 should decrease at TS by reason of the inner sharper peaks in RDFs (Figure 4a and c) while that around H5 might slightly increase because of the lack of unimolecularity (Figure 4b). As a whole, both contributions make the entropy at TS, $S^{\ddagger}$, decrease somewhat or keep almost constant, as a joint result by the two, that is, eq 3.9.

However, in Figure 2a one can recognize that the FE value of the ● curve at R(N1−H5) = 1.512 Å is ca. 2.5 kcal/mol smaller than that of the ▲ curve: $\Delta A^{\ddagger}_{\mathrm{FEG}} < \Delta A^{\ddagger}_{\mathrm{COSMO}}$. Taking into account this result in the FEG calculation, it is plausible to anticipate that the entropic contribution $T\Delta S^{\ddagger}_{\mathrm{FEG}}$ to the FE of activation $\Delta A^{\ddagger}_{\mathrm{FEG}}$ must be relatively small enough to keep the following inequality

$$\Delta A^{\ddagger}_{\mathrm{FEG}} = \Delta U^{\ddagger}_{\mathrm{FEG}} - T\Delta S^{\ddagger}_{\mathrm{FEG}} < \Delta H^{\ddagger}_{\epsilon} = \Delta A^{\ddagger}_{\mathrm{COSMO}} \tag{3.10}$$

even if the contribution might have a negative value, cf., eq 3.9. In other words, it can be noted that the present FEG research would expect that, in the ammonia ionization reaction in aqueous solution eq 3.7, the microscopic SIE stabilization at TS should play a predominant role in evaluating the FE of activation $\Delta A^{\ddagger}_{\mathrm{FEG}}$.

3.4. Free Energy of Activation for NH_3 Ionization Reaction − Theory versus Experiment. To evaluate the accuracy of the present approximation adopted in the FEG method, we have compared the theoretical FE of activation $\Delta A^{\ddagger}_{f}$ of the ammonia ionization reaction with the experimental one. The former value obtained by the FEG method was estimated to be 14.7 kcal/mol (300 K), which was estimated by the FE change $\Delta A^{\ddagger}_{\mathrm{FEG}}$ between the FE value at the SS (R(N1−H5) = 1.812 Å)[14] and that at the TS structure obtained in this work (R(N1−H5) = 1.512 Å) (Figure 2a). To estimate the experimental value of

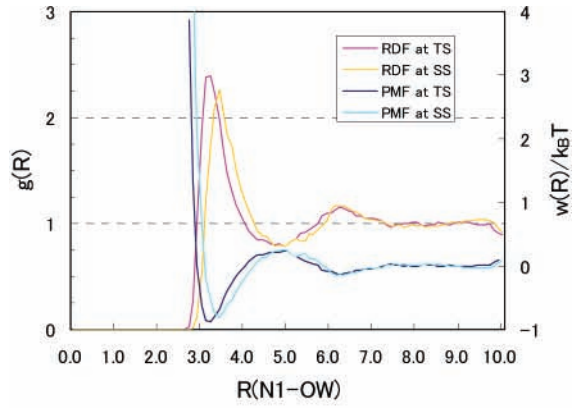

(a)

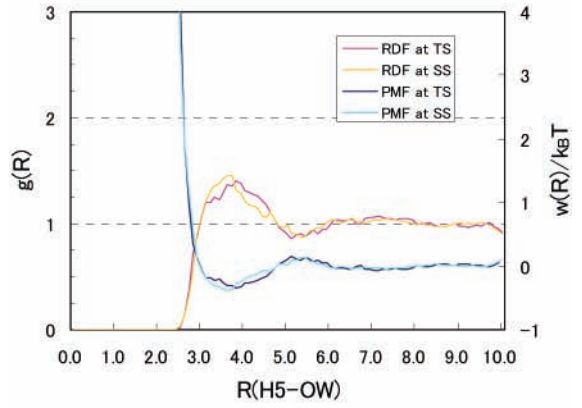

(b)

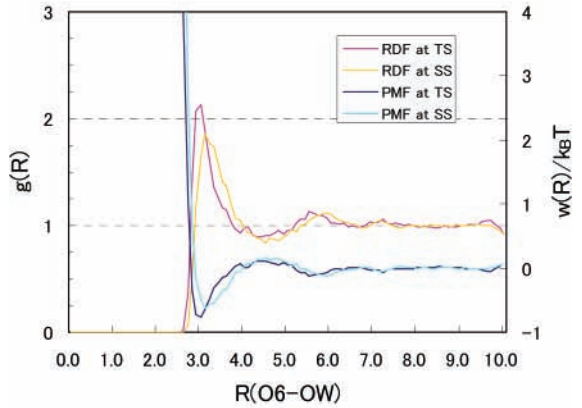

(c)

Figure 4. Radial distribution functions $g(R)$ and potentials of mean force $w(R)$ at the transition state (R(N1−H5) = 1.512 Å) and the stable state (R(N1−H5) = 1.812 Å) for (a) R(N1−OW), (b) R(H5−OW), and (c) R(O6−OW). $w(R)$s are drawn in the unit of k_BT (T = 300 K).

FE of activation, we consider the following equilibrium formula

$$NH_3 + H_2O \underset{k_b}{\overset{k_f}{\rightleftharpoons}} NH_4^+ + OH^- \qquad (3.11)$$

where k_f and k_b are the forward and backward rate constant, respectively, for the ammonia ionization reaction in aqueous solution. By Arrhenius formula, k_f is expressed within the TS theory (TST) as follows[60−62]

$$k_f^{TST} = \frac{k_B T}{h} \exp(-\Delta A_f^{\ddagger}/RT) \qquad (3.12)$$

where $\Delta A_f^{\ddagger}$ is the FE of activation in the forward reaction and R is the universal gas constant. Because the experimental value of k_f was reported to be 6×10^5 sec^{-1} at 295 K,[33] $\Delta A_f^{\ddagger}$ can be estimated to be 9.57 kcal/mol, which is in quite good agreement with the present theoretical estimation of 14.7 kcal/mol derived by the FEG method. It is true that a difference of 5.13 kcal/mol might be large between the theoretical value and the experimental one, which is referred to as $\Delta\Delta A_f^{\ddagger T-E}$ hereafter. However, it should be worth mentioning that because there are possible proton tunneling effects, intrinsically accounted for in the experimental value, but absent from the present calculated (classical) value, a tunneling correction could be one of the important reasons for the difference and would decrease the calculated barrier and, then, the agreement should become in fact even better.

Further, from the viewpoint of the electronic-state calculation level, taking into consideration three energy values of the bare $H_3N\cdots H_2O$ pair at R(N1−H5) = 1.512 Å, that is, 28.65 kcal/mol (PM3), 24.23 kcal/mol (B3LYP/6-31G(d)), and 26.34 kcal/mol (MP2/6-31G(d)), respectively, one can understand that the present estimation should be quite reasonable to conclude that the present application of the FEG method to the ammonia ionization process was accomplished successfully. First of all, it is because the energy difference between PM3 and B3LYP/6-31G(d) or between PM3 and MP2/6-31G(d), that is, 4.42 or 2.31 kcal/mol, was almost the same amount as 5.13 kcal/mol, which means that $\Delta\Delta A_f^{\ddagger T-E}$ might be originating mainly in the quality difference of electronic state calculations for the reactants themselves. Second, although one could not compensate the whole deviation $\Delta\Delta A_f^{\ddagger T-E}$ only with either energy difference between PM3 and B3LYP/6-31G(d) or that between PM3 and MP2/6-31G(d), the TS dipole moment 5.834 or 6.082 D at B3LYP/6-31G(d) or MP2/6-31G(d) is larger than 5.027 D at PM3, and it is, therefore, conjectured that the dielectric stabilization in the former two should be comparatively larger than that in the latter and might balance reasonably for the remaining amount of the deviation $\Delta\Delta A_f^{\ddagger T-E}$. Finally, it should be worth stating that the present effective QM/MM Hamiltonian eq 2.2 for the PM3/TIP3P combination was calibrated to provide the same interaction energy for the B3LYP/TIP3P combination using the full B3LYP/6-31G(d) interaction energy.[34] Thus, it can be concluded that the estimation would become about 10.28 kcal/mol if we took 24.23 kcal/mol, that is, the B3LYP/6-31G(d) value, as the better total energy V_S for the bare $H_3N\cdots H_2O$ pair. In fact, the value 10.28 kcal/mol agrees much more properly with the experimental value of 9.57 kcal/mol for the FE of activation in the ionization process.

4. Concluding Remarks

In this study, for the ionization process of ammonia in water, *full-atomic* TS geometry optimization has been performed theoretically by the FEG method, calculating the FE profiles in aqueous solution along the reaction coordinate R(N1−H5). The TS structure that does *not* exist in the gas phase was determined theoretically, *for the first time*, in aqueous solution, and the ammonia ionization process was understood to deviate largely in aqueous solution from that in the gas phase. The average RMS force at the optimized TS structure resulted in 0.0086 hartree/bohr, which was satisfactorily compared with previous values that were obtained in several applications of the FEG method in aqueous solution. Further, it was also observed that the dipole moment becomes larger with the ionization progress even after the TS. From this observation, it can be said that the solute polarization makes the solute potential energy itself

destabilized if the solute were in the gas phase, but the solute is stabilized *free-energetically* in aqueous solution by ambient water molecules, the microscopic SIE showing a relatively larger contribution than the microscopic SE in the ammonia ionization reaction in aqueous solution.

In addition, the FE of activation for ionization was evaluated by the FEG method and was discussed by comparing it with the experimental one obtained on the basis of TST expression. As far as nonquantal treatments are concerned, the present estimation of 14.7 kcal/mol is in good agreement with the experimental one, 9.57 kcal/mol, and it was concluded that the application of the FEG method to the ammonia ionization process was accomplished reasonably. The FEG method must provide us with a theoretical basis not only for discussing the application limit of TST, especially in solution,[60−64] but also for numerically examining, in real systems, the Kramers−Grote−Hynes theory that was proposed and developed rather qualitatively in 1980s[65] and has been analyzed almost within the quadratic approximation for the sake of analytical tractability.[66] We are now studying such theoretical advances in solution chemistry from the dynamic point of view in connection to the FEG methodology.

Acknowledgment. We thank Professor William L. Hase for his kind and important comments and unchanging warmhearted encouragements. The present article was originally intended to be our contribution to his JPC Festschrift issue on the occasion of his 60th birthday although it could not be accomplished for several reasons. In addition, we also thank Professor Manuel F. Ruiz-López for his kind and valuable comments at the early stage of the research. This work was supported partly by a Grant-in-Aid for Science Research from the Ministry of Education, Culture, Sport, Science and Technology in Japan and also by a Grant-in-Aid for the 21st Century COE Program "Frontiers in Computational Science" at Nagoya University.

References and Notes

(1) Amovili, C.; Barone, V.; Cammi, R.; Cances, E.; Cossi, M.; Mennucci, B.; Pomelli, C. S.; Tomasi, J. *Adv. Chem. Phys.* **1999**, *32*, 227.

(2) Gao, J.; Xia, X. *J. Am. Chem. Soc.* **1993**, *115*, 9667.

(3) Gao, J. *Acc. Chem. Res.* **1996**, *29*, 298.

(4) Maseras, F.; Morokuma, K. *J. Comput. Chem.* **1995**, *16*, 1170.

(5) Vreven, T.; Morokuma, K. *J. Comput. Chem.* **2000**, *16*, 1419.

(6) Torrent, M.; Vreven, T.; Musaev, D. G.; Morokuma, K.; Farkas, Ö.; Schlegel, H. B. *J. Am. Chem. Soc.* **2002**, *124*, 192.

(7) Sewell, T. D.; Thompson, D. L.; Gezelter, J. D.; Miller, W. H. *J. Chem. Phys.* **1992**, *193*, 512.

(8) Yamataka, H.; Aida, M.; Dupuis, M. *Chem. Phys. Lett.* **1999**, *300*, 583.

(9) Okuyama-Yoshida, N.; Nagaoka, M.; Yamabe, T. *Int. J. Quantum Chem.* **1998**, *70*, 95.

(10) Nagaoka, M.; Okuyama-Yoshida, N.; Yamabe, T. *J. Phys. Chem. A* **1998**, *102*, 8202.

(11) Okuyama-Yoshida, N.; Nagaoka, M.; Yamabe, T. *J. Phys. Chem. A* **1998**, *102*, 285.

(12) Okuyama-Yoshida, N.; Kataoka, K.; Nagaoka, M.; Yamabe, T. *J. Chem. Phys.* **2000**, *113*, 3519.

(13) Hirao, H.; Nagae, Y.; Nagaoka, M. *Chem. Phys. Lett.* **2001**, *348*, 350.

(14) Nagae, Y.; Oishi, Y.; Naruse, N.; Nagaoka, M. *J. Chem. Phys.* **2003**, *119*, 7972.

(15) Nagaoka, M. *Bull. Korean Chem. Soc.* **2003**, *24*, 805.

(16) (a) Chandler, D. *Introduction to Modern Statistical Mechanics*; Oxford: New York, 1987. (b) Nagaoka, M.; Okuno, Y.; Yoshida N.; Yamabe, T. *Int. J. Quantum Chem.* **1994**, *51*, 519.

(17) Singh, U. C.; Kollman, P. A. *J. Comput. Chem.* **1986**, *7*, 718.

(18) Bash, P. A.; Field, M. J.; Karplus, M. *J. Am. Chem. Soc.* **1987**, *109*, 8092.

(19) Field, M. J.; Bash, P. A.; Karplus, M. *J. Comput. Chem.* **1990**, *11*, 700.

(20) (a) Warshel, A.; Levitt, M. *J. Mol. Biol.* **1976**, *103*, 227. (b) Warshel, A. *Computer Modeling of Chemical Reactions in Enzymes and Solutions*; Wiley: New York, 1991.

(21) Galván, I. F.; Sánchez, M. L.; Martín, M. E.; Olivares del Valle, F. J.; Aguilar, M. A. *J. Chem. Phys.* **2003**, *118*, 255.

(22) Galván, I. F.; Martín, M. E.; Aguilar, M. A. *J. Comput. Chem.* **2004**, *25*, 1227.

(23) *Kagaku Binran*, 4th ed.; The Chemical Society of Japan: Maruzen, Tokyo, 1993.

(24) Ogasawara, N.; Horimoto, N.; Kawai, M. *J. Chem. Phys.* **2000**, *112*, 8229.

(25) Hara, Y.; Hashimoto, N. T.; Nagaoka, M. *Chem. Phys. Lett.* **2001**, *348*, 107.

(26) Hashimoto, N. T.; Hara, Y.; Nagaoka, M. *Chem. Phys. Lett.* **2001**, *350*, 141.

(27) Shinohara, H.; Nagashima, U.; Tanaka, H.; Nishi, N. *J. Chem. Phys.* **1985**, *83*, 4183.

(28) Herbine, P.; Dyke, T. R. *J. Chem. Phys.* **1985**, *83*, 3768.

(29) Bertie, J. E.; Shehata, M. R. *J. Chem. Phys.* **1985**, *83*, 1449.

(30) Donaldson, D. J. *J. Phys. Chem. A* **1999**, *103*, 62.

(31) Vanderzee, C. E.; King, D. L.; Wadsö, I. *J. Chem. Thermodyn.* **1972**, *4*, 685.

(32) Olofsson, G. *J. Chem. Thermodyn.* **1975**, *7*, 507.

(33) Friess, S. L.; Lewis, E. S.; Weissberger, A. Investigation of Rate and Mechanism of Reactions. *Technique of Organic Chemistry*; Interscience: 1963; Vol.8-II,

(34) Luque, F. J.; Reuter, N.; Cartier, A.; Ruiz-López, M. F. *J. Phys. Chem. A* **2000**, *104*, 10923.

(35) (a) Klamt, A.; Schüürmann, G. *J. Chem. Soc., Perkin Trans.* **1993**, *2*, 799. (b) Klamt, A. COSMO-RS From *Quantum Chemistry to Fluid Phase Thermodynamics and Drug Design*; Elsevier: Amsterdam, 2005.

(36) Zwanzig, R. W. *J. Chem. Phys.* **1954**, *22*, 1420.

(37) Singh, U. C.; Brown, F. K.; Bash, P. A.; Kollman, P. A. *J. Am. Chem. Soc.* **1987**, *109*, 1607.

(38) McIver, J. W., Jr.; Komornicki, A. *Chem. Phys. Lett.* **1971**, *10*, 303.

(39) McIver, J. W., Jr.; Komornicki, A. *J. Am. Chem. Soc.* **1972**, *94*, 2625.

(40) Cheng, A.; Stanton, R. S.; Vincent, J. J.; van der Vaart, A.; Damodaran, K. V.; Dixon, S. L.; Hartsough, D. L.; Mori, M.; Best, S. A.; Monard, G.; Garcia, M.; Van Zant, L. C.; Merz, K. M., Jr. *ROAR 2.0*; The Pennsylvania State University: University Park, PA, 1999.

(41) Pearlman, D. A.; Case, D. A.; Caldwell, J. W.; Ross, W. S.; Cheatham, T. E., III; Ferguson, D. M.; Seibel, G. L.; Singh, U. C.; Weiner, P. K.; Kollman, P. A. *AMBER 6.0*; Unversity of California: San Francisco, CA, 1995.

(42) van Gunsteren, W. F.; Berendsen, H. J. C. *Mol. Phys.* **1977**, *34*, 1311.

(43) Anderson, H. C. *J. Comput. Phys.* **1983**, *52*, 24.

(44) Martyna, G. J.; Klein, M. L. *J. Chem. Phys.* **1992**, *97*, 2635.

(45) Stewart, J. J. P. *J. Comput. Chem.* **1989**, *10*, 209.

(46) Stewart, J. J. P. *J. Comput. Chem.* **1989**, *10*, 221.

(47) Stewart, J. J. P. *MOPAC 7.0*, QCPE no. 455.

(48) Jorgensen, W. L.; Chandrasekhar, J.; Madula, J. D.; Impey, R. W.; Klein, M. L. *J. Chem. Phys.* **1983**, *79*, 926.

(49) Cummins, P. L.; Gready, J. E. *J. Comput. Chem.* **1997**, *18*, 1496.

(50) (a) Becke, A. D. *J. Chem. Phys.* **1993**, *98*, 5648. (b) Becke, A. D. *J. Chem. Phys.* **1992**, *96*, 2155. (c) Lee, C.; Yang, W.; Parr, R. G. *Phys. Rev. B* **1988**, *37*, 785.

(51) (a) St.-Amant, A.; Cornell, W. D.; Kollman, P. A.; Halgren, T. A. *J. Comput. Chem.* **1995**, *16*, 1483. (b) De Proft, F.; Martin, J. M. L.; Geerlings, P. *Chem. Phys. Lett.* **1996**, *250*, 393. (c) Soliva, R.; Orozco, M.; Luque, F. J. *J. Comput. Chem.* **1997**, *18*, 980. (d) Soliva, R.; Luque, F. J.; Orozco, M. *Theor. Chem. Acc.* **1997**, *98*, 42.

(52) (a) Topol, I. A.; Burt, S. K.; Rashin, A. A. *Chem. Phys. Lett.* **1995**, *247*, 112. (b) Sim, F.; St.-Amant, A.; Papsi, I.; Salahub, D. R. *J. Am. Chem. Soc.* **1992**, *114*, 4391. (c) Hobza, P.; Šponer, J.; Reschel, T. J. *J. Comput. Chem.* **1995**, *16*, 1315. (d) Colominas, C.; Teixidó, J.; Cemelí, J.; Luque, F. J.; Orozco, M. J. *J. Phys. Chem. B* **1998**, *102*, 2269. (e) Colominas, C.; Luque, F. J.; Orozco, M. J. *J. Phys. Chem. A* **1999**, *103*, 6200.

(53) (a) Thompson, M. A. *J. Phys. Chem.* **1996**, *100*, 14492. (b) Bakowies, D.; Thiel, W. *J. Comput. Chem.* **1996**, *17*, 87. (c) Vasylyev, V. V.; Bliznyuk, A. A.; Voityuk, A. A. *Int. J. Quantum Chem.* **1992**, *44*, 897.

(54) (a) Ford, G. P.; Wang, B. *J. Comput. Chem.* **1993**, *14*, 1101. (b) Cummins, P. L.; Gready, J. E. *J. Comput. Chem.* **1999**, *20*, 1028. (c) Théry, V.; Rinaldi, D.; Rivail, J. L.; Maigret, B.; Ferenczy, G. G. *J. Comput. Chem.* **1994**, *15*, 269.

(55) (a) Bernal-Uruchurtu, M. I.; Martins-Costa, M. T.; Millot, C.; Ruiz-López, M. F. *J. Comput. Chem.* **2000**, *21*, 572. (b) Harb, W.; Bernal-Uruchurtu, M. I.; Ruiz-López, M. F. *Theor. Chem. Acc.* **2004**, *112*, 204. (c) Monard, G.; Bernal-Uruchurtu, M. I.; van der Vaart, A.; Merz, K. M., Jr.; Ruiz-López, M. F. *J. Phys. Chem. A* **2005**, *109*, 3425.

(56) Frisch, M. J.; Trucks, G. W.; Schlegel, H. B.; Scuseria, G. E.; Robb, M. A.; Cheeseman, J. R.; Montgomery, J. A., Jr.; Vreven, T.; Kudin, K. N.; Burant, J. C.; Millam, J. M.; Iyengar, S. S.; Tomasi, J.; Barone, V.; Mennucci, B.; Cossi, M.; Scalmani, G.; Rega, N.; Petersson, G. A.; Nakatsuji, H.; Hada, M.; Ehara, M.; Toyota, K.; Fukuda, R.; Hasegawa, J.; Ishida, M.; Nakajima, T.; Honda, Y.; Kitao, O.; Nakai, H.; Klene, M.; Li, X.; Knox, J. E.; Hratchian, H. P.; Cross, J. B.; Bakken, V.; Adamo, C.; Jaramillo, J.; Gomperts, R.; Stratmann, R. E.; Yazyev, O.; Austin, A. J.; Cammi, R.; Pomelli, C.; Ochterski, J. W.; Ayala, P. Y.; Morokuma, K.; Voth, G. A.; Salvador, P.; Dannenberg, J. J.; Zakrzewski, V. G.; Dapprich, S.; Daniels, A. D.; Strain, M. C.; Farkas, O.; Malick, D. K.; Rabuck, A. D.; Raghavachari, K.; Foresman, J. B.; Ortiz, J. V.; Cui, Q.; Baboul, A. G.; Clifford, S.; Cioslowski, J.; Stefanov, B. B.; Liu, G.; Liashenko, A.; Piskorz, P.; Komaromi, I.; Martin, R. L.; Fox, D. J.; Keith, T.; Al-Laham, M. A.; Peng, C. Y.; Nanayakkara, A.; Challacombe, M.; Gill, P. M. W.; Johnson, B.; Chen, W.; Wong, M. W.; Gonzalez, C.; Pople, J. A. *Gaussian 03*, revision B.05; Gaussian, Inc.: Wallingford, CT, 2004.

(57) Gao, J.; Xia, X. *Science* **1992**, *258*, 631.

(58) Tu, Y.; Laaksonen, A. *Chem. Phys. Lett.* **2000**, *329*, 283.

(59) Coutinho, K.; Guedes, R. C.; Cabral, B. J. C.; Canuto, S. *Chem. Phys. Lett.* **2003**, *369*, 345.

(60) Arrhenius, S. *Z. Phys. Chem.* **1889**, *4*, 226.

(61) Glasstone, S.; Laidler, K. J.; Eyring, H. *The Theory of Rate Processes*; McGraw-Hill: New York, 1941.

(62) Steinfeld, J. I.; Francisco, J. S.; Hase, W. L. *Chemical Kinetics and Dynamics*; Prentice-Hall: New York, 1989.

(63) Truhlar, D. G.; Hase, W. L.; Hynes, J. T. *J. Phys. Chem.* **1989**, *87*, 2664.

(64) Truhlar, D. G.; Garrett, B. C.; Klippenstein, S. J. *J. Phys. Chem.* **1996**, *100*, 12771.

(65) Hynes, J. T. In *Theory of Chemical Reaction Dynamics*; Baer, M., Ed.; Boca Raton, Florida, 1985; Vol. IV.

(66) *Activated Barrier Crossing*; Fleming, G. R., Hänggi, P., Eds.; World Scientific: Singapore, 1993.